Effect of radiation and non-Maxwellian electron distribution on relaxation processes in an atmospheric cesium seeded argon plasma

Eindhoven
University of Technology
the Netherlands

Department of Electrical Engineering

Effect of Radiation and Non-Maxwellian Electron Distribution on Relaxation Processes in an Atmospheric Cesium Seeded Argon Plasma

By
C.A. Borghi, A. Veefkind and J.M. Wetzer

EUT Report 82-E-124
ISBN 90-6144-124-2
March 1982

Eindhoven University of Technology Research Reports
EINDHOVEN UNIVERSITY OF TECHNOLOGY

Department of Electrical Engineering
Eindhoven The Netherlands

EFFECT OF RADIATION AND NON-MAXWELLIAN ELECTRON DISTRIBUTION ON RELAXATION PROCESSES IN AN ATMOSPHERIC CESIUM SEEDED ARGON PLASMA

By

C.A. Borghi
A. Veefkind
J.M. Wetzer

EUT Report 82-E-124
ISBN 90-6144-124-2

Eindhoven
March 1982

Abstract

A model, describing the time dependent behaviour of a noble gas MHD generator plasma, has been set up. With this model it is possible to calculate the relaxation for ionization or recombination as a response to a stepwise temperature development, once the initial and final conditions are given.

In the model radiative transitions and a deviation from Maxwellian electron distribution are included. Radiation causes an enhancement of both the ionization relaxation time and the recombination relaxation time. A non-Maxwellian electron distribution results in an increase of the relaxation time for an ionizing plasma because of an underpopulation of the high energy electrons. A decrease of the relaxation time for a recombining plasma is caused by an overpopulation of high energy electrons. The relaxation time is strongly dependent on the seed ratio and the temperature step.

Borghi, C.A., A. Veefkind and J.M. Wetzer
EFFECT OF RADIATION AND NON-MAXWELLIAN ELECTRON DISTRIBUTION ON RELAXATION PROCESSES IN AN ATMOSPHERIC CESIUM SEEDED ARGON PLASMA.
Department of Electrical Engineering, Eindhoven University of Technology, 1982.
EUT Report 82-E-124

Address of the authors:

Group Direct Energy Conversion,
Department of Electrical Engineering,
Eindhoven University of Technology,
P.O. Box 513,
5600 MB EINDHOVEN,
The Netherlands

Contents

LIST OF SYMBOLS

A_{ij}	spontaneous emission coefficient
A'_{ij}	net emission coefficient
$A_{\lambda i}$	rate integral for radiative recombination
$A'_{\lambda i}$	net rate integral for radiative recombination
a_o	radius of the first Bohr orbit of hydrogen
f	reduced density value defining the characteristic time
$f(\varepsilon_e)$	electron energy distribution
$f^b(\varepsilon_e)$	electron energy distribution bulk electrons
$f^t(\varepsilon_e)$	electron energy distribution tail electrons
g_i	degeneracy of atomic level i
h	Planck's constant
K_{ij}	rate integral for electronic (de)excitation from atomic level i to atomic level j
K_i	partial rate integral
$K_{i\lambda}$	rate integral for electronic ionisation from atomic level i
$K'_{i\lambda}$	effective rate integral for electronic ionisation from atomic level i
$K_{\lambda i}$	rate integral for three body recombination to atomic level i
$K'_{\lambda i}$	effective rate integral for three body recombination to atomic level i
k	Boltzmann's constant
m_e	electron mass
n_{Ar}	Argon density
n_{Cs}	Cesium density
$n_e(t)$	electron density
$n_i(t)$	population density of atomic level i
$\tilde{n}_e$	reduced electron density
$\tilde{n}_i$	reduced population density of atomic level i

R	Rydberg's constant
s	seed ratio
T_e	electron temperature (bulk)
T_t	electron temperature tail
T_{eo}, T_{to}	temperature at $t<o$
$T_{e\infty}$, $T_{t\infty}$	temperature at $t \geq o$
ΔT	temperature step at $t=o$
t	time
v_e	electron velocity
β_{ij}	radiation escape factor of radiative transition from atomic level i to atomic level j
$\beta_{\lambda i}$	radiation escape factor for radiative recombination to atomic level i
ε_e	electron energy
ε_{ij}	energy difference between atomic levels i and j
$\varepsilon_{i\lambda}$	ionisation energy of atomic level i
ξ_i	number of equivalent electrons in atomic level i
$\sigma_i(\varepsilon_e, \Delta\varepsilon)$	cross section for loss of energy greater than or equal to $\Delta\varepsilon$ by one incoming electron of energy ε_e colliding with a bound electron in atomic level i
$\sigma_{ij}(\varepsilon_e)$	cross section for excitation from atomic level i to to atomic level j by one incoming electron of energy ε_e
$\sigma_{i\lambda}(\varepsilon_e)$	cross section for ionisation from atomic level i by one incoming electron of energy ε_e
τ	characteristic time for relaxation

1. Introduction

In order to attain a nonequilibrium regime in noble gas MHD generator plasmas, the populations of the excited states of the seed atoms and the electron density must be elevated above their equilibrium values corresponding to the gas temperature by electronic collisional processes (1). Generally in relaxation models it is assumed that the thermalization energy due to electron-electron collisions is much larger than the energy transfer due to elastic and non-elastic collisions with heavy particles. Consequently a Maxwellian function is assumed to describe the energy distribution of the electrons (1,2). For values of the electron density lower than 10^{19} m^{-3} the energy loss due to excitations to the first excited state becomes of the same order as the energy transfer from low to high energetic electrons (3). As a result the electron energy distribution will deviate from a Maxwellian one.

In this study a noble gas Cs seeded plasma is investigated. The model includes radiative transitions and the possibility of a deviation from the Maxwellian electron energy distribution. The two electron group model is used to describe the electron distribution (3,4). The different contributions of the electrons belonging to the two groups to the non-elastic collisions are then considered. For ionizing plasmas, where excitation to the first excited state represents the principal energy loss, the tail of the electron distribution is considered to be depleated($T_t < T_e$). For recombining plasmas, where de-excitation from the first excited state represents the principal energy gain, the tail of the electron distribution is considered to be overpopulated ($T_t > T_e$).

2. Theoretical Model

2.1. Basic assumptions

In the model only Cs atoms are supposed to be excited and to be ionized while all Argon atoms are supposed to be in the ground state. Further, it is assumed that the time required for the electron energy distribution to relax to its final condition, is short compared with the ionizational relaxation time. Consequently the final electron energy distribution is assumed to be established at t=o and maintained constant in time. The initial population of excited states and electron density are obtained from the stationary solution of the model for a given initial electron energy distribution (at t < o). When a Maxwellian electron energy distribution is assumed and the radiative transitions are neglected, the values of the population density and electron density given by the stationary solution of the model are equal to the values given by Saha relation.

2.2. Electron distribution function

The two electron group model (3,4) is used to describe the energy distribution of the electrons. The electrons are divided in two groups: bulk electrons with energies smaller than ε_{12} (excitation energy of the first excited level of the Cs atom), and tail electrons with energies higher than ε_{12}. Two Maxwellian distribution functions are assumed to describe the two electron energy groups: $f^b(\varepsilon_e)$ for the bulk electrons with an effective temperature T_e, and $f^t(\varepsilon_e)$ for the tail electrons with an effective temperature T_t.

$$f^b(\varepsilon_e) = 2\left[\frac{\varepsilon_e}{\pi(kT_e)^3}\right]^{\frac{1}{2}} \exp\left(-\frac{\varepsilon_e}{kT_e}\right), \qquad (1)$$

$$f^t(\varepsilon_e) = 2\left[\frac{\varepsilon_e}{\pi(kT_t)^3}\right]^{\frac{1}{2}} \exp\left(-\frac{\varepsilon_e}{kT_t}\right), \qquad (2)$$

Here ε_e the energy of the electrons and k is Boltzmann's constant.

The electron distribution function defined by eq. 1,2, fulfils the normalization condition with a good accuracy as is discussed in Ref. 4.

2.3. Atomic model

An atomic model of Cesium having 10 bound states is used. Each state is characterised by its principal quantum number and orbital momentum (see Table 1). Energy levels higher than the 10th (7 D, ε_{io}=3.23 eV) are assumed to be in instantaneous Saha equilibrium with the free electrons.

The collisional processes taken into account are inelastic electron-atom collisions viz. excitation, de-excitation, ionization and three-body recombination. Because of the lack of experimental values of cross sections for electron induced excitation or ionization from intermediate levels of the Cs-atom, the formulas derived by Gryziński (1965) on the basis of a semi-classical model, are used (5). According to Gryziński's theory the cross section $\sigma_i(\varepsilon_e, \Delta\varepsilon)$ for loss of energy greater than or equal to $\Delta\varepsilon$ by one incoming electron of energy ε_e colliding with a bound electron in the i-th level, is given by

$$\sigma_i \; (\varepsilon_e,\Delta\varepsilon) = 4\pi a_o^2 \; (\frac{R}{\Delta\varepsilon})^2 \; \xi_i \; g(u,v) \; , \qquad (3)$$

where

$$g\;(u,v) = \frac{u-1}{u^2} \; . \; (\frac{u}{u+v})^{3/2} \; (1-\frac{1}{u})^{\frac{v}{v+1}} \{1+ \frac{2v}{3}(1-\frac{1}{2u}) \; \ln \; [e+(\frac{u-1}{v})^{\frac{1}{2}}]\} \qquad (4)$$

Here a_o = 5.29 x 10^{-11}m is the radius of the first Bohr orbit for hydrogen, R = 13.6 eV is Rydberg's constant, ξ_i is the number of equivalent electrons in the i-th level, $u = \varepsilon_e/\Delta\varepsilon$ and $v = \varepsilon_{i\lambda}/\Delta\varepsilon$ where $\varepsilon_{i\lambda}$ is the ionisation energy for the i-th level, and e = 2.7183. Excitation from level i to level j is obtained when the mimimum energy loss is larger than the excitation energy ε_{ij} but smaller than the excitation energy of the next level, $\varepsilon_{i,j+1}$, hence

$$\sigma_{ij} \; (\varepsilon_e) = \sigma_i \; (\varepsilon_e,\varepsilon_{ij}) - \sigma_i \; (\varepsilon_e,\varepsilon_{i,j+1}) \qquad (5)$$

Similarly the cross section for ionization from level i is

$$\sigma_{i\lambda}(\varepsilon_e) = \sigma_i(\varepsilon_e, \varepsilon_{i\lambda}) , \qquad (6)$$

The dominating radiative processes are 6S - 6P resonance radiation and radiative recombination into the levels 6P and 5D. Other radiative transitions are taken into account but appear to have a negligible effect on populations and electrondensity. Oscillatorstrengths are taken from Fabry (6), cross-sections for radiative recombination from Norcross & Stone (7).

2.4. Rate integrals

The rate integrals for excitation, de-excitation, ionization and recombination are calculated for collisions with electrons having an energy distribution as defined in sec. 2.1. The excitation rate integral K_{ij} is defined in terms of the excitation cross section σ_{ij} by

$$K_{ij} = \int_{\varepsilon_{ij}}^{\infty} f(\varepsilon_e)\, \sigma_{ij}(\varepsilon_e)\, v_e(\varepsilon_e)\, d\varepsilon_e , \qquad (7)$$

where $f(\varepsilon_e)$ is the electron distribution function and v_e is the electron velocity $v_e = (2\varepsilon_e/m_e)^{½}$ where m_e is the electron mass. Using the excitation cross section from the previous section eq. 7 gives

$$K_{ij} = K_i(\varepsilon_{i,j}) - K_i(\varepsilon_{i,j+1}) , \qquad (8)$$

where $K_i(\varepsilon_{i,j})$ is defined as

$$K_i(\varepsilon_{i,j}) = \int_{\varepsilon_{i,j}}^{\infty} f(\varepsilon_e)\, \sigma_i(\varepsilon_e, \varepsilon_{i,j})\, v_e(\varepsilon_e)\, d\varepsilon_e \qquad (9)$$

When the distribution function is given by eqs. 1 and 2, two cases are distinguished for the calculation of $K_i(\varepsilon_{ij})$.

case a: $\varepsilon_{ij} < \varepsilon_{12}$, then

$$K_i(\varepsilon_{ij}) = \int_{\varepsilon_{ij}}^{\varepsilon_{12}} f^b(\varepsilon_e)\, \sigma_i(\varepsilon_e, \varepsilon_{ij})\, v_e(\varepsilon_e)\, d\varepsilon_e \; +$$

$$\int_{\varepsilon_{12}}^{\infty} f^t (\varepsilon_e) \, \sigma_i (\varepsilon_e, \varepsilon_{ij}) \, v_e (\varepsilon_e) \, d\varepsilon_e \, , \qquad (10)$$

case b: $\varepsilon_{12} \leq \varepsilon_{ij}$, then

$$K_i (\varepsilon_{ij}) = \int_{\varepsilon_{ij}}^{\infty} f^t (\varepsilon_e) \, \sigma_i (\varepsilon_e, \varepsilon_{ij}) \, v_e (\varepsilon_e) \, d\varepsilon_e \, , \qquad (11)$$

The ionization rate integral is.

$$K_{i\lambda} = K_i (\varepsilon_{i\lambda}) \, , \qquad (12)$$

and $K_i (\varepsilon_{i\lambda})$ is expressed by eqs. 10 and 11 where ε_{ij} is replaced by $\varepsilon_{i\lambda}$.

The de-excitation and recombination rates are derived from detailed balancing as

$$K_{ji} = K_{ij} \left(\frac{n_i}{n_j}\right)^* \, , \qquad (13)$$

$$K_{\lambda i} = K_{i\lambda} \left(\frac{n_i}{n_e^2}\right)^* \, , \qquad (14)$$

where

$$\left(\frac{n_i}{n_j}\right)^* = \frac{g_i}{g_j} \exp (\varepsilon_{ij}/kT_e) \, , \qquad (15)$$

$$\left(\frac{n_i}{n_e^2}\right)^* = \frac{1}{2} \left(\frac{h^2}{2\pi m_e kT_e}\right)^{3/2} g_i \exp (\varepsilon_{i\lambda}/kT_e) \qquad (16)$$

Furthermore in eqs. 13 and 14, K_{ij} and $K_{i\lambda}$ are calculated for a Maxwellian distribution function at the bulk temperature T_e (i.e. in eqs. 10 and 11 $f^t (\varepsilon_e)$ is replaced by $f^b (\varepsilon_e)$. The effect of the non-Maxwellian distribution is neglected for the de-excitation and the recombination collisions as these processes are dominated by the bulk electrons, infact their energy threshold is zero and the thermal energy of the electrons is sufficiently small compared to the threshold energy. In a similar way as described for exitation and ionization processes, the rate integral for radiative recombination to atomic level i, $A_{\lambda i}$, is calculated from

$$A_{\lambda i} = \int_0^\infty f\ (\varepsilon_e)\ \sigma_{\lambda i}\ (\varepsilon_e)\ v_e\ (\varepsilon_e)\ d\varepsilon_e\ , \tag{17}$$

2.5. Time dependent continuity equations

In general the continuity equation for atoms in state i can be written as

$$\frac{\partial n_i}{\partial t} = \left(\frac{\partial n_i}{\partial t}\right)_{coll.rad.} + \nabla .\ (n_i \underline{v}_i)\ , \tag{18}$$

In our model diffusive effects are not taken into account. Then the right hand side of eq. (18) reduces to collisional and radiative terms:

$$\frac{\partial n_i}{\partial t} = \left(\frac{\partial n_i}{\partial t}\right)_{coll.rad.} = n_e\ \left[\sum_{j\neq i} n_j K_{ji} - n_i \sum_{j\neq i} K_{ij} - n_i K_{i\lambda} + n_e^2 K_{\lambda i} + n_e A^1_{\lambda i}\right] + \sum_{j>i} n_j A^1_{ji} - n_i \sum_{j<i} A^1_{ij}\ , \tag{19}$$

where charge neutrality is assumed.

$A^1_{\lambda i}$ is the net rate integral for radiative recombination and A^1_{ij} is the net emission coëfficient that take into account the corresponding absorption processes.

Using the radiation escape factors $\beta_{\lambda i}$ and β_{ij}, $A^1_{\lambda i}$ and A^1_{ij} are defined as follows:

$$A^1_{\lambda i} = A_{\lambda i}\ \beta_{\lambda i}\ , \tag{20}$$

$$A^1_{ij} = A_{ij}\ \beta_{ij}\ , \tag{21}$$

The plasma is considered optically thin to recombination radiaton thus $\beta_{\lambda i} \simeq 1$.

Using Holstein's theory (8) β_{6S-6P} is calculated for the plasma considered, yielding values in the order of 0.01. All other radiative transitions appeared to have a negligible effect even in case of complete radiation escape (β=1).

The assumption of Saha equilibrium for levels higher than 7D is realised by adjusting $K_{i\lambda}$ and $K_{\lambda i}$. According to Bates et al. (9) these rate integrals should then be replaced by $K^1_{i\lambda}$ and $K^1_{\lambda i}$ as follows:

$$K^1_{i\lambda} = K_{i\lambda} + \sum_{j=n}^{\infty} K_{ij} , \qquad (22)$$

$$K^1_{\lambda i} = (n_i/n_e^2) * K^1_{i\lambda} \qquad (23)$$

where n is the number of levels taken into account. The converging character of the summation leeds to a value for $K^1_{i\lambda}$ which is in good agreement with the rate integral $K_{i\lambda}$ oblained when using $\varepsilon_{1,n+1}$(=3.33eV) as the effective ionization energy. It should be noted however that this effective ionization energy is used only for evaluating $K^1_{i\lambda}$, and that for all other processes involving the ionization energy the real value is used.

The resulting set of stiff differential equations is numerically solved with a Curtiss-Hirschfelder method (10), while n_e is simultaneously calculated from

$$n_e = n_{cs} - \sum_1^n n_i , \qquad (24)$$

in which n_{cs} is the cesium concentration.

3. Results and discussion

3.1 Conditions

The development of the electron temperature is simulated by a step function at t = o. Further, when the influence of a non-Maxwellian distribution is considered, the tail of the electron distribution is assumed to have a discontinuity at energy ε_{12}. The behavior in time of the electron energy distribution is given by a step function of the bulk and tail temperatures as follows:

$$T_e = T_{eo},\ T_t = T_{to} \text{ for } t < o\ , \qquad (25.a)$$

$$T_e = T_{e\infty},\ T_t = T_{t\infty} \text{ for } t \geq o\ , \qquad (25.b)$$

The initial conditions are given by eq. 25.a. The values of T_{eo} and of T_{to} determine the stationary solution of the model from which the electron density n_e (o) and the population density n_i (o) are derived. The rate integrals in the time dependant equations (eq. 19), are calculated from the values of $T_{e\infty}$ and $T_{t\infty}$ given by the final conditions (eq. 25.b).

The electron density and the excited state densities are calculated for three different sets of conditions:

1) Radiation is neglected.
   The electron distribution function is Maxwellian.
   - Initial conditions (t < o): $T_e = T_t = T_{eo}$.
   - Final conditions (t $\geq$ o): $T_e = T_t = T_{e\infty}$.
2) Radiation is taken into account.
   The electron distribution function is Maxwellian.
   - Initial conditions $T_e = T_t = T_{eo}$.
   - Final conditions $T_e = T_t = T_{e\infty}$.
3) Radiation is taken into account.
   The electron distribution function is non-Maxwellian.
   With regard to the electron distribution three different possibilities are considered:
   a. Initial conditions $T_e = T_{eo}$, $T_t = T_{to}$.
      Final conditions $T_e = T_t = T_{e\infty}$.

b. Initial conditions $T_e = T_t = T_{eo}$
Final conditions $T_e = T_{e\infty}$, $T_t = T_{t\infty}$

c. Initial conditions $T_e = T_{eo}$, $T_t = T_{to}$
Final conditions $T_e = T_{e\infty}$, $T_t = T_{t\infty}$

When a non-Maxwellian electron distribution function is considered, the ionizing plasma case is distinguished from the recombining plasma case.

For ionizing plasmas T_t is assumed to be smaller than T_e due to the excitation losses (3). For recombining plasmas T_t is assumed to be larger than T_e as the de-exitations and the recombinations, as far as not balanced by the excitations and the ionizations, cause extra population of the tail of the electron distribution function.

The results of the calculations are plotted for reduced values of the electron density $\tilde{n}_e$ and of the population density $\tilde{n}_i$ defined as:

$$\tilde{n}_k = \frac{n_k(t) - n_k(o)}{n_k(\infty) - n_k(o)} , \qquad (26)$$

where $k = e,1,2 \ldots, n$ and $n_k(\infty)$ stands for the stationary solution of the model at $T_e = T_{e\infty}$ and $T_t = T_{t\infty}$.

3.2. Influence of radiation and distribution function

In figure 1.A a comparison is presented of the results of the model where radiations are neglected (case 1), with the results of the model that takes radiation into account (case 2) for an ionizing plasma subjected to a temperature step from T_{eo} = 2100K to $T_{e\infty}$ = 2300K. When radiation is neglected $\tilde{n}_2$ and $\tilde{n}_3$ reach quickly their final values. The development becomes slower as the level becomes higher. The electron density time dependance is similar to the time dependance of the high levels ($\tilde{n}_e(t) \simeq \tilde{n}_i(t)$, $i = 8,9,10$). Resonance radiation is a loss of particles for level 2, the population of which increases slower. As a consequence the whole relaxation process becomes slower. In figure 1.B a comparison is given of the results with the same conditions for a recombining plasma with T_{eo} = 2300K and $T_{e\infty}$ = 2100K. The model that includes radiation gives a larger difference between the initial and final values of the electron density and of the population densities. As a consequence the whole relaxation process is retarded in comparison with the results given by the model which neglects radiation. Only the development of $\tilde{n}_2(t)$ remaines appreciably fast due to resonance radiation.

In figure 2.A a comparison of the results of the model including radiation with and without (case 2 and 3 resp.) deviations from Maxwellian distribution is shown. For case 2: $T_{eo} = T_{to} = 2100K$, $T_{e\infty} \equiv T_{t\infty} = 2300K$. For case 3: $T_{eo} = 2100K$, $T_{to} = 2000K$, $T_{e\infty} = 2300K$ and $T_{t\infty} = 2200K$. When a tail depleated electron energy distribution is considered, the difference between initial and final densities increases and the values of the rate integrals for excitations between levels with a large energy separation decrease. As a result the relaxation process is retarded. The decreased values of K_{12} and K_{13} are followed by a further depressed development of $\tilde{n}_2(t)$ and $\tilde{n}_3(t)$ which gets closer to the development of the other population densities and to the electron density. A comparison between the results of the two models of case 2 and case 3 for a recombining plasma are presented in figure 2.B. For the first one $T_{eo} = T_{to} = 2300K$ and $T_{e\infty} = T_{t\infty} = 2100K$. For the second one $T_{eo} = 2300K$, $T_{to} = 2400K$, $T_{e\infty} = 2100K$, $T_{t\infty} = 2200K$. In the non-Maxwellian case $T_t > T_e$. As a consequence $\tilde{n}_2$, $\tilde{n}_3$ and then $\tilde{n}_e$ develop faster.

The time dependance of the electron density for the cases of the figures 1 and 2 and for the three different possibilities in which the non-Maxwellian case is divided, are plotted in figure 3. The ionizing case is shown in figure 3.A. The recombining case is shown in figure 3.B. Comparing the resulting $\tilde{n}_e(t)$ for a non-Maxwellian initial condition and a non-Maxwellian final condition, it can be noted that the former shows a more pronounced deviation from the Maxwellian case.

In figure 4 the values of the characteristic time for the electron density relaxation as a function of the seed ratio s are plotted for different conditions. The seed ratio is defined by $s = n_{cs}/n_{ar}$, where n_{cs} is the density of cesium and n_{Ar} is the density of argon. The argon density is $n_{Ar} = 7 \times 10^{24} m^{-3}$, corresponding to a gas pressure of 1 atm. at a gas temperature of 1000K. The characteristic time τ for the relaxation of the electron density is defined by the following expression:

$$\tilde{n}_e(\tau) = f \qquad (27)$$

In the ionizing plasma case (figure 4.A) f is taken as $1 - e^{-1} = 0.632$. For decreasing seed fraction, τ increases. This effect becomes more pronounced at low seed fractions when the model includes radiation or a non-Maxwellian distribution. For a recombining plasma two characteristic times are defined. One is connected to the early relaxation of $\tilde{n}_e$ (t) and is defined by eq. 27 for f = 0.632. The other one is defined by eq. 27 for f = 0.99 and accounts for the late relaxation of $\tilde{n}_e$ (t). The dependance on seed ratio of the characteristic times for early and late relaxation of a recombining plasma is shown in figure 4.B.

The influence of the temperature step on the characteristic time is shown in figure 5. For an ionizing plasma (figure 5.A) T_{eo} = 2100K, $T_{e\infty} = T_{eo} + \Delta T$. In the non-Maxwellian case only the begin condition is assumed non-Maxwellian with T_{eo} = 2100K, T_{to} = 2000K, while $T_{e\infty} = T_{t\infty} = T_{eo} + \Delta T$. The characteristic time decreases for increasing values of ΔT. For a recombining plasma (figure 5.B) T_{eo} = 2300K, $T_{e\infty} = T_{eo} - \Delta T$. In the non-Maxwellian case T_{eo} = 2300K, T_{to} = 2400K, $T_{e\infty} = T_{t\infty} = T_{eo} - \Delta T$. The characteristic time for the early relaxation decreases for increasing ΔT while the characteristic time for the late relaxation increases for increasing ΔT.

4. Conclusions

In the preceding section a comparison between relaxation processes with and without radiation and non-Maxwellian energy distribution has been made. Radiation causes lower densities of electrons and excited atoms in initial-, and final state as well as enhancement of de-excitation. Both effects result in an increase of the ionization relaxation time. The recombination relaxation time increases as well for the conditions considered because the effect of lower final values predominates the enhanced de-excitation. The effect of radiation is more pronounced at low seed ratio.

A non-Maxwellian final state has a smaller effect on the relaxation behaviour than an non-Maxwellian initial state. For an ionizing plasma the relaxation time increases in case of a non-Maxwellian distribution because the depleated tail causes lower initial values. For a recombining plasma the tail of the energy distribution is overpopulated, yielding a shorter relaxation time.

In all cases the relaxation time is strongly dependant on seed ratio and temperature step.

The effect of non-Maxwellian distribution, however, does not vary much in the ranges considered.

Acknowledgement

This work was performed as a part of the research program of the Shock Tube MHD project of the Group Direct Energy Conversion of the Eindhoven University of Technology.
The authors wish to express their gratitude to prof.dr. J.F. Uhlenbusch and ir. A.J.G. Manders for their contribution and fruitful discussions.

References

(1) Takeshita, T. and L.M. Grossman
EXCITATION AND IONIZATION PROCESSES IN NON-EQUILIBRIUM MHD PLASMAS.
In: Electricity from MHD, 1968. Proc. 4th Int. Symp. on Magnetohydrodynamic Electrical Power Generation; Warsaw, 24-30 July 1968. Vol. 1: Closed-cycle MHD with gaseous working fluids.
Vienna: International Atomic Energy Agency, 1968.
Proceedings series. P. 191-206.

(2) Bertolini, E., R. Toschi and I.R. McNab
RELAXATION PHENOMENA IN MPD GENERATORS.
In: Electricity from MHD. Proc. 3rd Int. Symp. on Magnetohydrodynamic Electrical Power Generation; Salzburg, 4-8 July 1966. Vol. 1.
Vienna: International Atomic Energy Agency, 1966.
Proceedings series. P. 533-545.

Zauderer, B.
EXPERIMENTAL STUDY OF THE RELAXATION PROCESS AND THE MAGNITUDE OF NON-THERMAL IONIZATION IN AN MHD GENERATOR.
Ibid., p. 239-252.

(3) Borghi, C.A.
DISCHARGES IN THE INLET REGION OF A NOBLE GAS MHD GENERATOR.
Ph.D. Thesis. Eindhoven University of Technology, 1982.

(4) Vriens, L.
ENERGY BALANCE IN LOW-PRESSURE GAS DISCHARGES.
J. Appl. Phys., Vol. 44(1973), p. 3980-3989.

(5) Gryziński, M.
CLASSICAL THEORY OF ATOMIC COLLISIONS. I: Theory of inelastic collisions.
Phys. Rev. A, Vol. 138(1965), p. 336-358.

(6) Fabry, M.
THEORETICAL AND EXPERIMENTAL DETERMINATIONS OF CESIUM OSCILLATOR STRENGTHS.
J. Quant. Spectrosc. & Radiat. Transfer, Vol. 16(1976), p. 127-135.

(7) Norcross, D.W. and P.M. Stone
RADIATIVE RECOMBINATION IN CESIUM.
J. Quant. Spectrosc. & Radiat. Transfer, Vol. 6(1966), p. 277-290.

(8) Holstein, T.
IMPRISONMENT OF RESONANCE RADIATION IN GASES. II.
Phys. Rev., Vol. 83(1951), p. 1159-1168.

(9) Bates, D.R., A.E. Kingston and R.W.P. McWhirter
RECOMBINATION BETWEEN ELECTRONS AND ATOMIC IONS.
I: Optically thin plasmas.
Proc. R. Soc. London Ser. A, Vol. 267(1962), p. 297-312.
II: Optically thick plasmas.
Ibid., Vol. 270(1962), p. 155-167.

(10) Gear, C.W.
NUMERICAL INITIAL VALUE PROBLEMS IN ORDINARY DIFFERENTIAL EQUATIONS.
Englewood Cliffs, N.J.: Prentice-Hall, 1971.
Prentice-Hall series in automatic computation

(11) Blom, J.H. and J.W.M.A. Houben
RELAXATION LENGTH CALCULATIONS IN Ar-Cs MIXTURES FOR ONE- AND TWO-DIMENSIONAL PRE-IONIZER GEOMETRIES.
In: Papers presented at the 5th Int. Conf. on Magnetohydrodynamic Electrical Power Generation; Munich, 19-23 April 1971. Vol. 2: Closed cycle plasma MHD systems.
Karlsruhe: Zentralstelle für Atomkernenergie-Dokumentation (ZAED), 1971. P. 65-79.

	Level	Energy (eV)	Degeneracy
	i	ε_{1i}	g_i
1.	6 S	0.00	2
2	6 P	1.42	6
3.	5 D	1.80	10
4.	7 S	2.30	2
5.	7 P	2.71	6
6.	6 D	2.80	10
7.	8 S	3.01	2
8.	4 F	3.03	14
9.	8 P	3.19	6
10	7 D	3.23	10
11.	ion	3.89	1

Table 1. Cesium atomic model with level energy ε_{1i}, and corresponding degeneracy g_i.

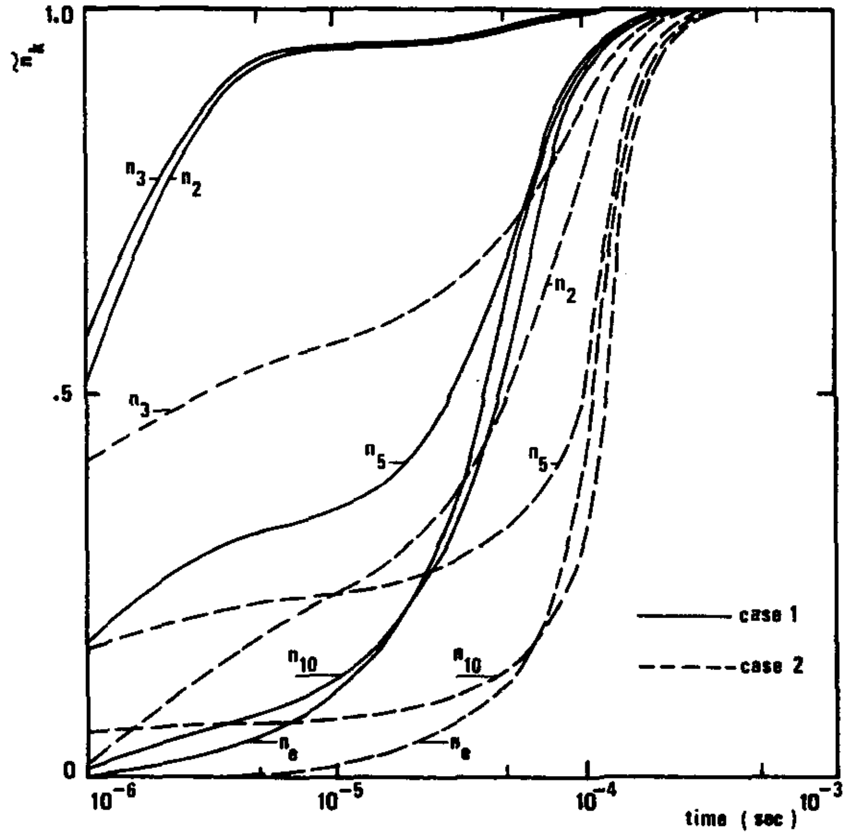

Figure 1.A.

Development in time of reduced densities in case of a Maxwellian distribution function, $n_{Cs} = 7.241 \times 10^{21}\ m^{-3}$.

Ionizing plasma, $T_{eo} = T_{to} = 2100\ K$, $T_{e\infty} = T_{t\infty} = 2300\ K$.

Case 1: No radiation included. Case 2: Radiation included.

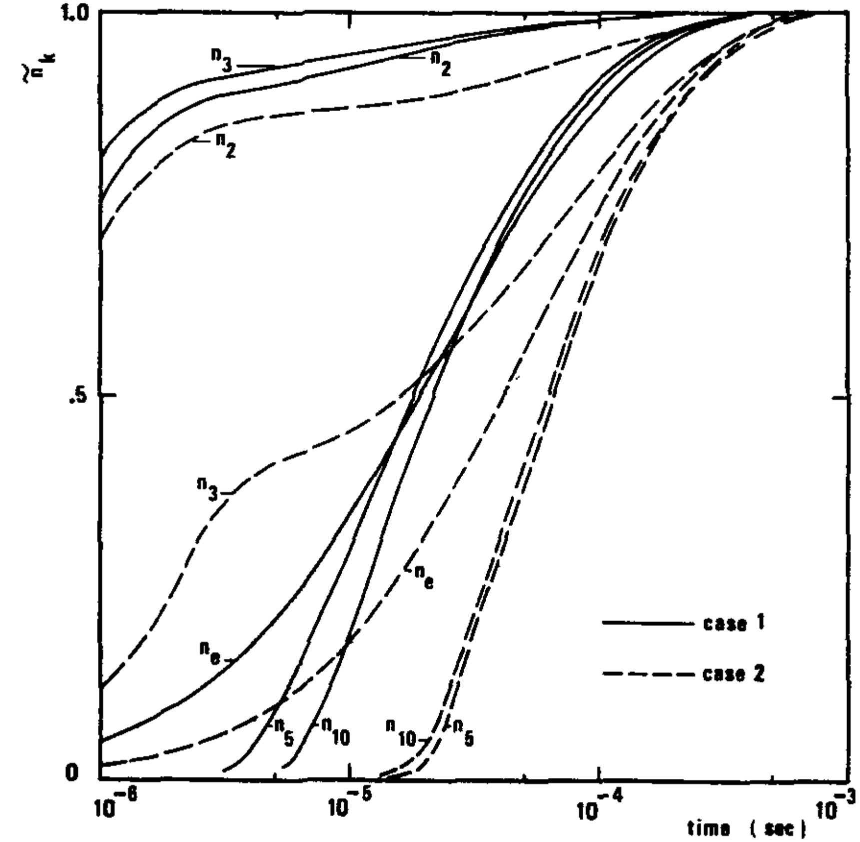

Figure 1.B.

Development in time of reduced densities in case of a Maxwellian distribution function, $n_{Cs} = 7.241 \times 10^{21}\ m^{-3}$.

Recombining plasma, $T_{eo} = T_{to} = 2300\ K$, $T_{e\infty} = T_{t\infty} = 2100\ K$.

Case 1: No radiation included. Case 2: Radiation included.

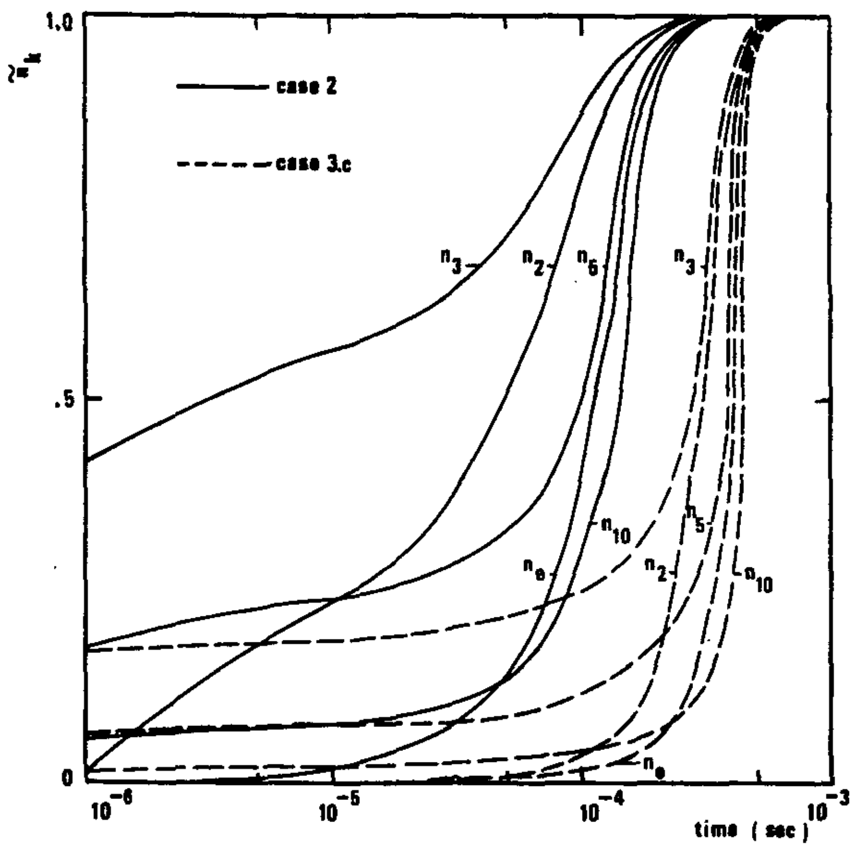

Figure 2.A.

Development in time of reduced densities, radiation included, with Maxwellian (case 2) and non-Maxwellian (case 3c) distribution function, $n_{Cs} = 7.241 \times 10^{21}\ m^{-3}$.

Ionizing plasma,

Case 2: $T_{eo} = T_{to} = 2100$ K, $T_{e\infty} = T_{t\infty} = 2300$ K.

Case 3c: $T_{eo} = 2100$ K, $T_{to} = 2000$ K, $T_{e\infty} = 2300$ K, $T_{t\infty} = 2200$ K.

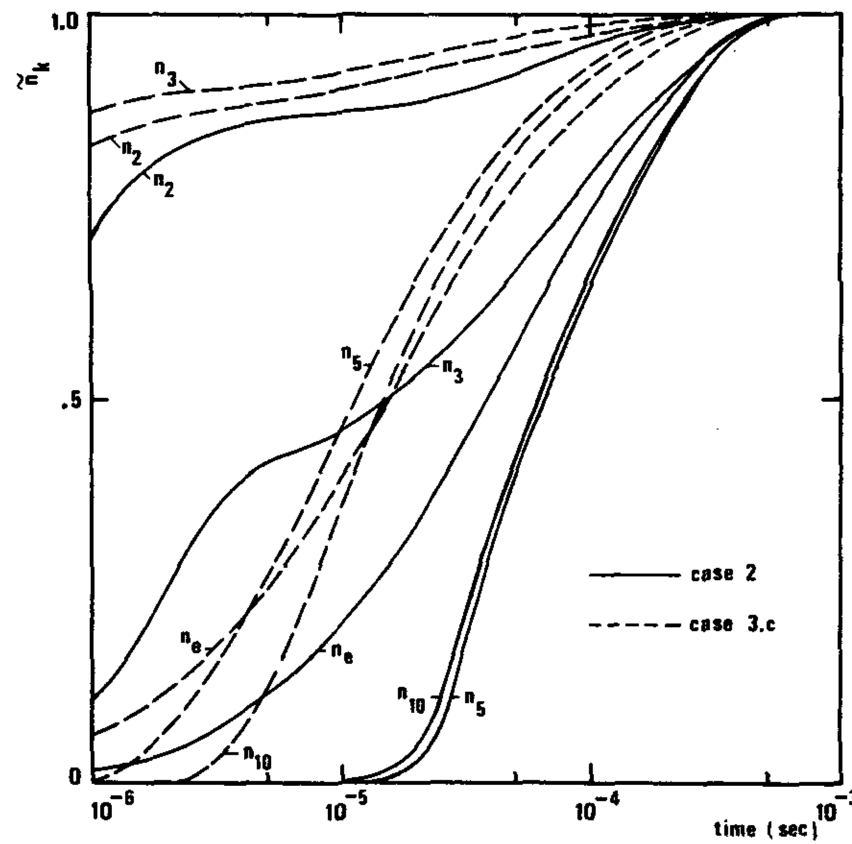

Figure 2.B.

Development in time of reduced densities, radiation included, with Maxwellian (case 2) and non-Maxwellian (case 3c) distribution function, $n_{Cs} = 7.241 \times 10^{21}\ m^{-3}$.

Recombining plasma,

Case 2: $T_{eo} = T_{to} = 2300$ K, $T_{e\infty} = T_{t\infty} = 2100$ K.

Case 3c: $T_{eo} = 2300$ K, $T_{to} = 2400$ K, $T_{e\infty} = 2100$ K, $T_{t\infty} = 2200$ K.

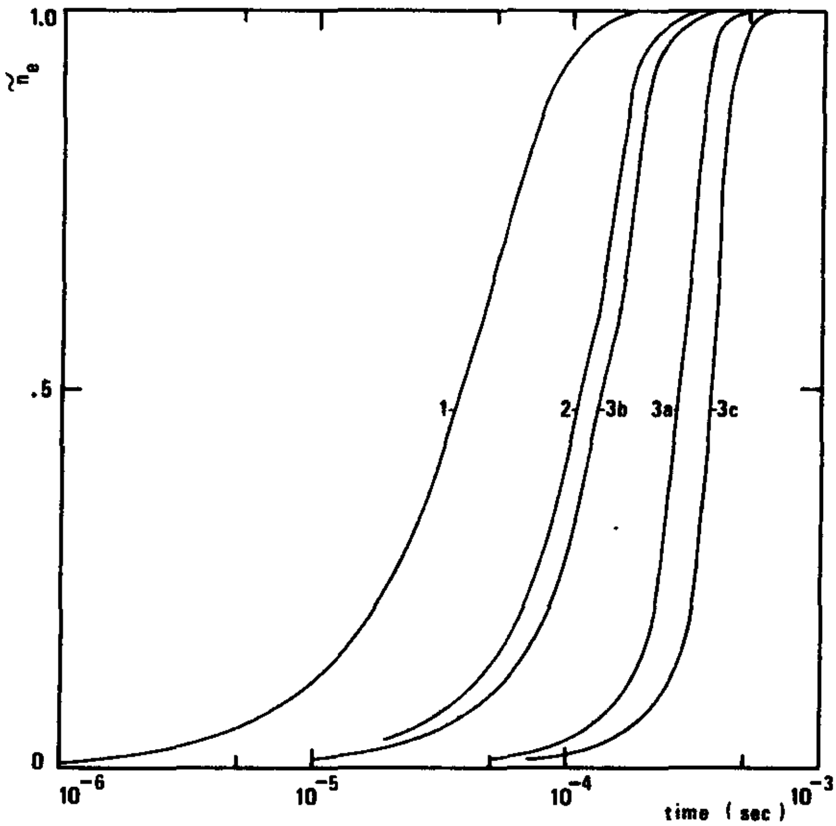

Figure 3.A.

Development in time of reduced electrondensity, $n_{Cs} = 7.241 \times 10^{21}\ m^{-3}$.

Case 1: No radiation included. Cases 2 and 3: Radiation included.

Ionizing plasma, $T_{eo} = 2100$ K, $T_{e\infty} = 2300$ K.

Case 1 and 2: $T_t = T_e$.

Case 3a. $T_{to} = 2000$ K $\quad T_{t\infty} = 2300$ K

3b. $T_{to} = 2100$ K $\quad T_{t\infty} = 2200$ K

3c. $T_{to} = 2000$ K $\quad T_{t\infty} = 2200$ K

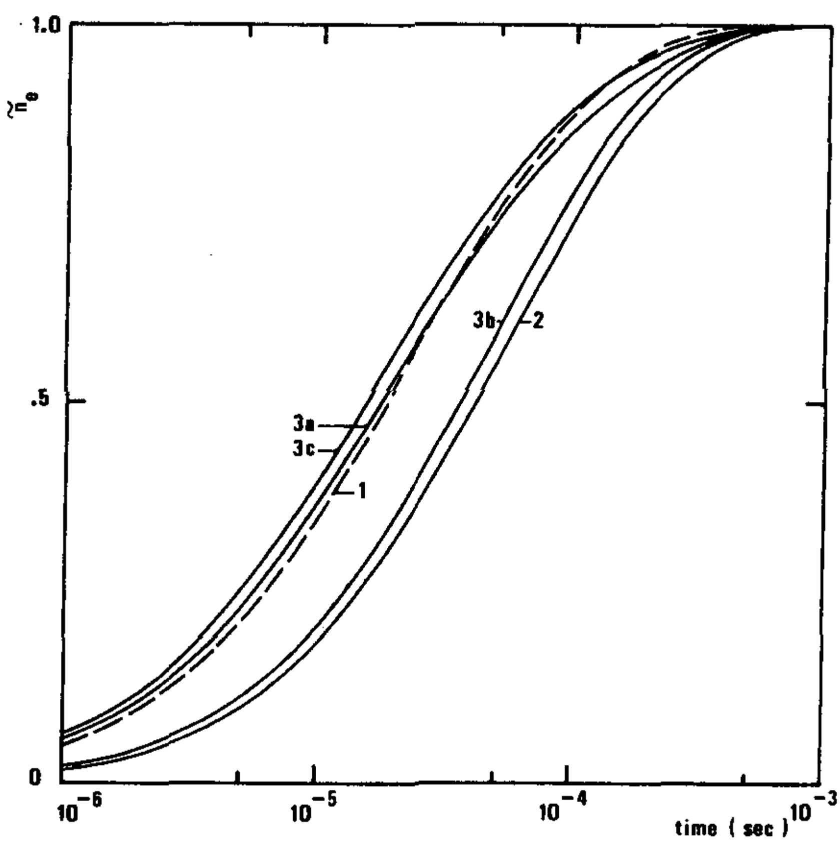

Figure 3.B.

Development in time of reduced electrondensity, $n_{Cs} = 7.241 \times 10^{21}\ m^{-3}$.

Case 1: No radiation included. Cases 2 and 3: Radiation included.

Recombining plasma, $T_{eo} = 2300$ K, $T_{e\infty} = 2100$ K.

Case 1 and 2: $T_t = T_e$.

Case 3a. $T_{to} = 2400$ K $\quad T_{t\infty} = 2100$ K

3b. $T_{to} = 2300$ K $\quad T_{t\infty} = 2200$ K

3c. $T_{to} = 2400$ K $\quad T_{t\infty} = 2200$ K

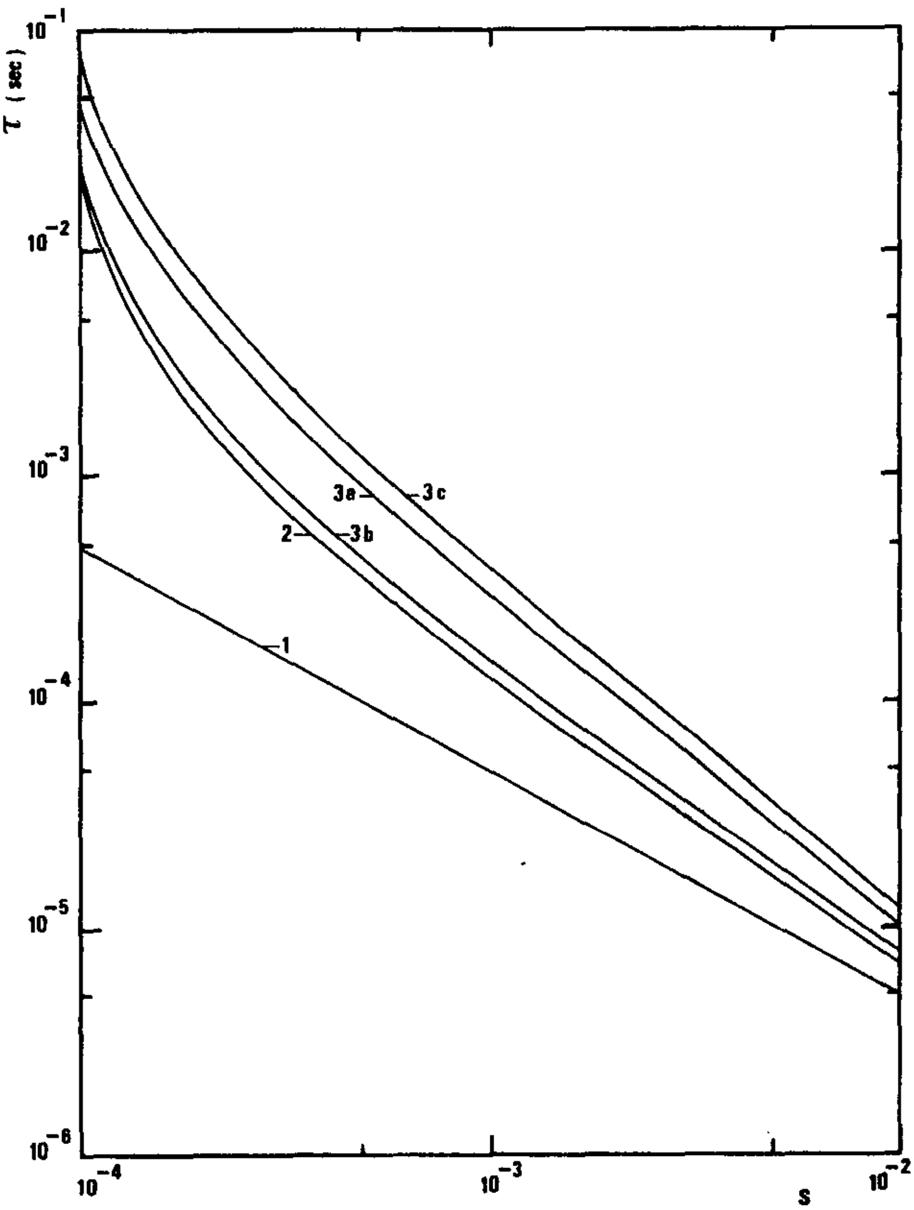

Figure 4.A.

Relaxation time for an ionizing plasma ($f = 1-e^{-1}$) as a function of seed ratio. Different cases like in figure 3.A.

$n_{Ar} = 7.2 \times 10^{24}\ m^{-3}$.

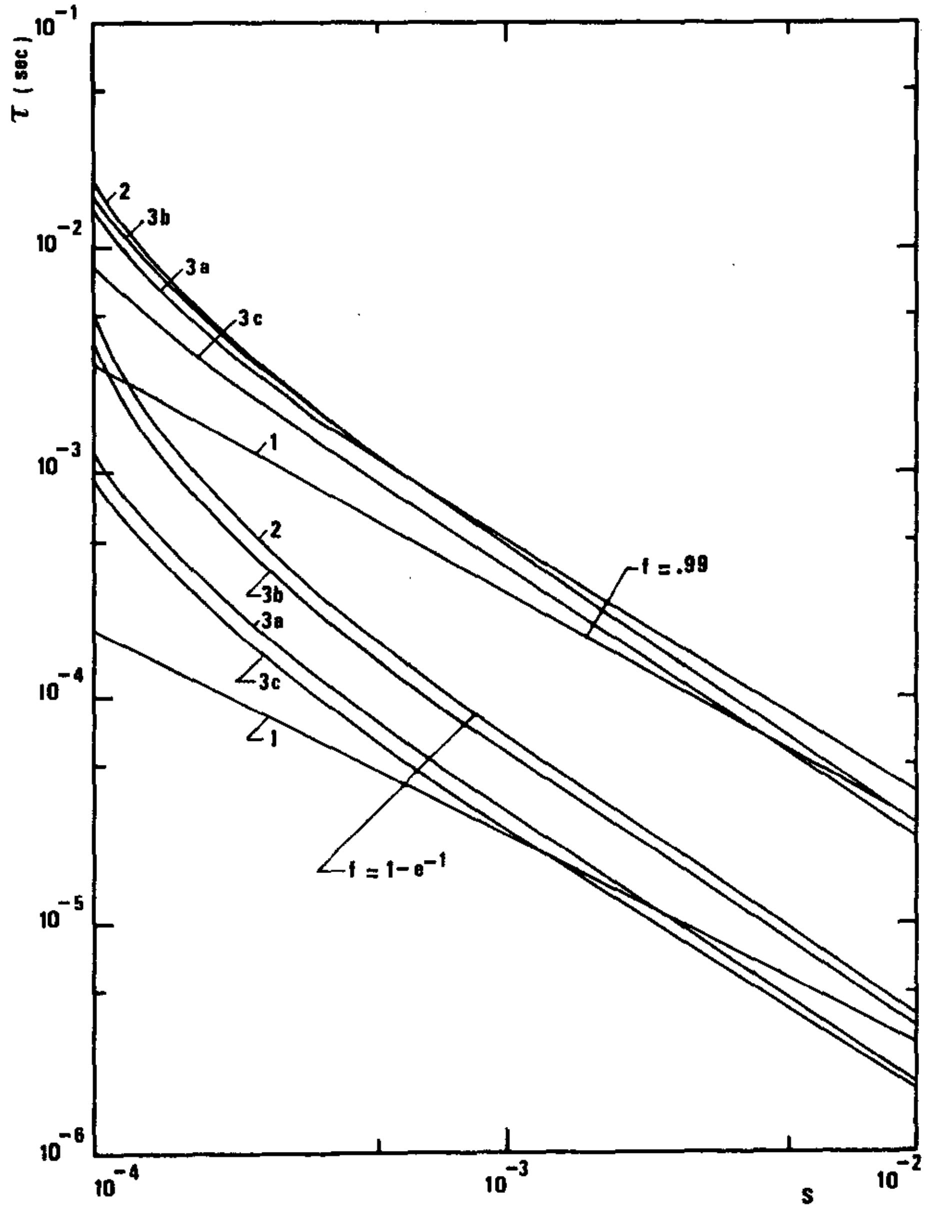

<u>*Figure 4.B.*</u>

Relaxation time for a recombining plasma (early relaxation: $f = 1\text{-}e^{-1}$; late relaxation: $f = 0{,}99$) as a function of seed ratio.

Different cases like in figure 3.B.

$n_{Ar} = 7.2 \times 10^{24}\ m^{-3}$.

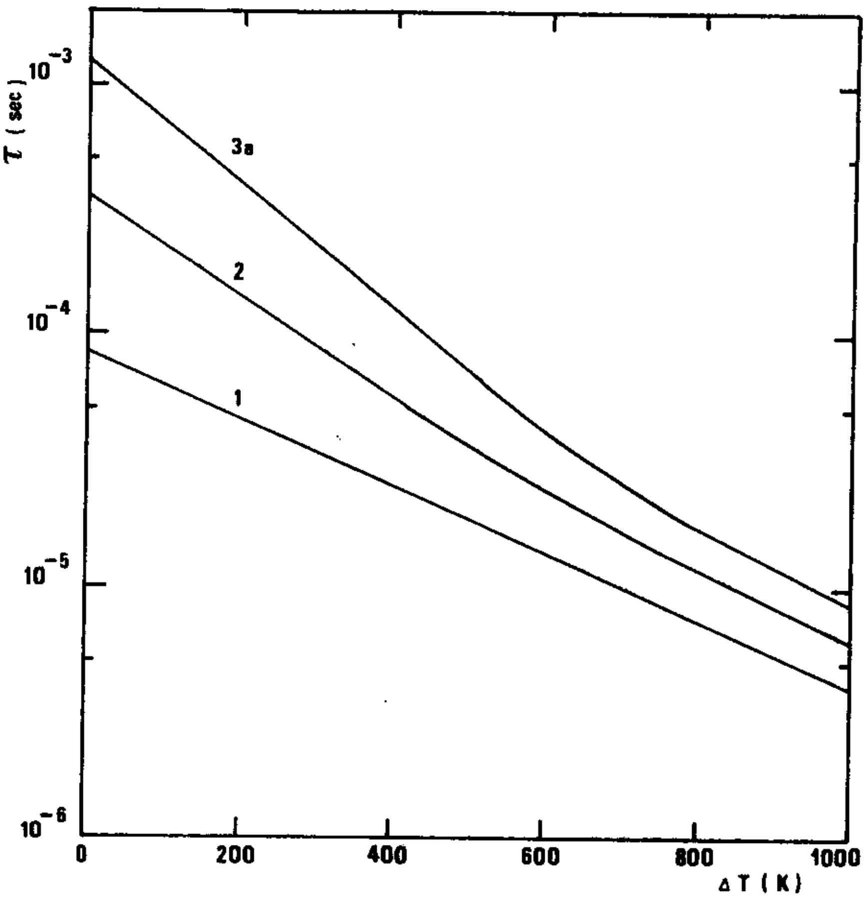

Figure 5.A.

Relaxation time as a function of temperature step, $n_{Cs} = 7.241 \times 10^{21}\ m^{-3}$.

Case 1: No radiation included.

Case 2 and 3a: Radiation included; $T_{e\infty} = T_{t\infty}$.

Ionizing plasma, $(f = 1-e^{-1})$, $T_{eo} = 2100$ K, $T_{e\infty} = T_{eo} + \Delta T$.

Case 1 and 2: $T_{to} = T_{eo}$.

Case 3a: $T_{to} = 2000$ K.

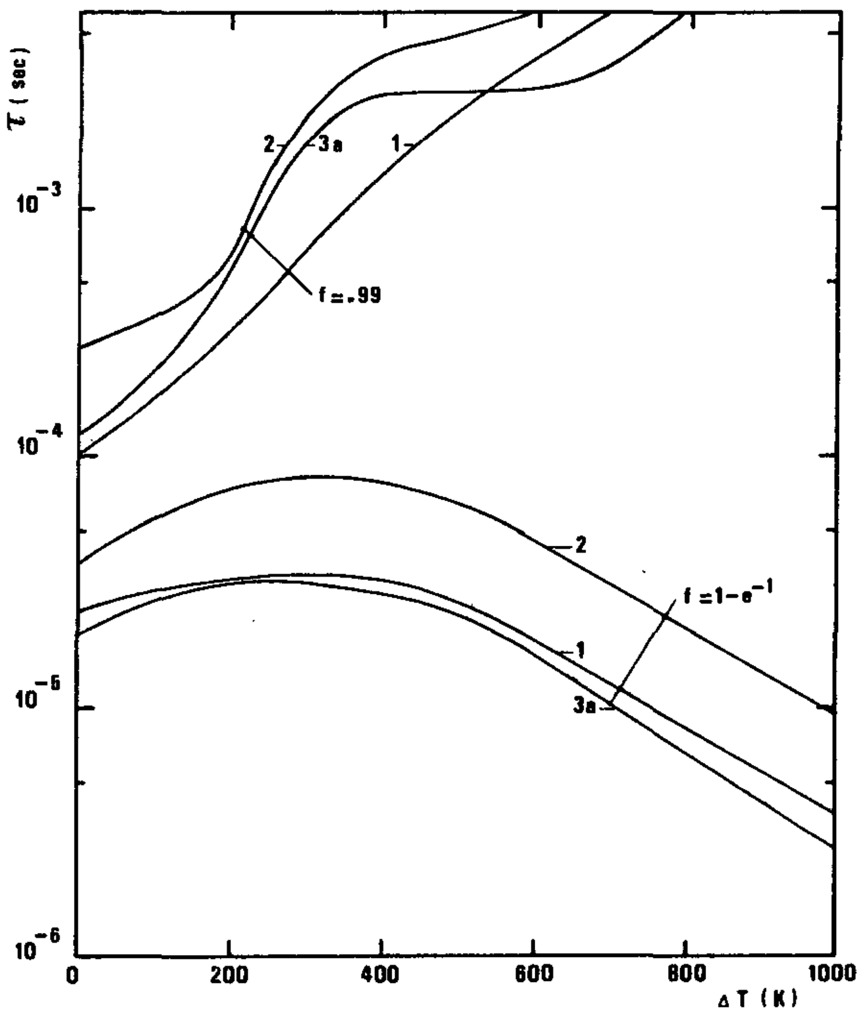

<u>*Figure 5.B.*</u>

Relaxation time as a function of temperature step, $n_{Cs} = 7.241 \times 10^{21}\ m^{-3}$.

Case 1: No radiation included.

Case 2 and 3a: Radiation included; $T_{e\infty} = T_{t\infty}$.

Recombining plasma, $T_{eo} = 2300\ K \quad T_e = T_{eo} - \Delta T$

$f = 1-e^{-1}$, *early relaxation*

$f = 0.99$, *late relaxation*

Case 1 and 2: $T_{to} = T_{eo}$.

Case 3a: $T_{to} = 2400$.

EINDHOVEN UNIVERSITY OF TECHNOLOGY
THE NETHERLANDS
DEPARTMENT OF ELECTRICAL ENGINEERING

Reports:

105) Videc, M.F.
STRALINGSVERSCHIJNSELEN IN PLASMA'S EN BEWEGENDE MEDIA: Een geometrisch-optische en een golfzonebenadering.
TH-Report 80-E-105. 1980. ISBN 90-6144-105-6

106) Hajdasiński, A.K.
LINEAR MULTIVARIABLE SYSTEMS: Preliminary problems in mathematical description, modelling and identification.
TH-Report 80-E-106. 1980. ISBN 90-6144-106-4

107) Heuvel, W.M.C. van den
CURRENT CHOPPING IN SF_6.
TH-Report 80-E-107. 1980. ISBN 90-6144-107-2

108) Etten, W.C. van and T.M. Lammers
TRANSMISSION OF FM-MODULATED AUDIOSIGNALS IN THE 87.5 - 108 MHz BROADCAST BAND OVER A FIBER OPTIC SYSTEM.
TH-Report 80-E-108. 1980. ISBN 90-6144-108-0

109) Krause, J.C.
SHORT-CURRENT LIMITERS: Literature survey 1973-1979.
TH-Report 80-E-109. 1980. ISBN 90-6144-109-9

110) Matacz, J.S.
UNTERSUCHUNGEN AN GYRATORFILTERSCHALTUNGEN.
TH-Report 80-E-110. 1980. ISBN 90-6144-110-2

111) Otten, R.H.J.M.
STRUCTURED LAYOUT DESIGN.
TH-Report 80-E-111. 1981. ISBN 90-6144-111-0

112) Worm, S.C.J.
OPTIMIZATION OF SOME APERTURE ANTENNA PERFORMANCE INDICES WITH AND WITHOUT PATTERN CONSTRAINTS.
TH-Report 80-E-112. 1980. ISBN 90-6144-112-9

113) Theeuwen, J.F.M. en J.A.G. Jess
EEN INTERACTIEF FUNCTIONEEL ONTWERPSYSTEEM VOOR ELEKTRONISCHE SCHAKELINGEN.
TH-Report 80-E-113. 1980. ISBN 90-6144-113-7

114) Lammers, T.M. en J.L. Manders
EEN DIGITAAL AUDIO-DISTRIBUTIESYSTEEM VOOR 31 STEREOKANALEN VIA GLASVEZEL.
TH-Report 80-E-114. 1980. ISBN 90-6144-114-5

115) Vinck, A.J., A.C.M. Oerlemans and T.G.J.A. Martens
TWO APPLICATIONS OF A CLASS OF CONVOLUTIONAL CODES WITH REDUCED DECODER COMPLEXITY.
TH-Report 80-E-115. 1980. ISBN 90-6144-115-3

EINDHOVEN UNIVERSITY OF TECHNOLOGY
THE NETHERLANDS
DEPARTMENT OF ELECTRICAL ENGINEERING

Reports:

EUT Reports are a continuation of TH-Reports.

116) Versnel, W.
THE CIRCULAR HALL PLATE: Approximation of the geometrical correction factor for small contacts.
TH-Report 81-E-116. 1981. ISBN 90-6144-116-1

117) Fabian, K.
DESIGN AND IMPLEMENTATION OF A CENTRAL INSTRUCTION PROCESSOR WITH A MULTIMASTER BUS INTERFACE.
TH-Report 81-E-117. 1981. ISBN 90-6144-117-X

118) Wang Yen Ping
ENCODING MOVING PICTURE BY USING ADAPTIVE STRAIGHT LINE APPROXIMATION.
EUT Report 81-E-118. 1981. ISBN 90-6144-118-8

119) Heijnen, C.J.H., H.A. Jansen, J.F.G.J. Olijslagers and W. Versnel
FABRICATION OF PLANAR SEMICONDUCTOR DIODES, AN EDUCATIONAL LABORATORY EXPERIMENT.
EUT Report 81-E-119. 1981. ISBN 90-6144-119-6.

120) Piecha, J.
DESCRIPTION AND IMPLEMENTATION OF A SINGLE BOARD COMPUTER FOR INDUSTRIAL CONTROL.
EUT Report 81-E-120. 1981. ISBN 90-6144-120-X

121) Plasman, J.L.C. and C.M.M. Timmers
DIRECT MEASUREMENT OF BLOOD PRESSURE BY LIQUID-FILLED CATHETER MANOMETER SYSTEMS.
EUT Report 81-E-121. 1981. ISBN 90-6144-121-8

122) Ponomarenko, M.F.
INFORMATION THEORY AND IDENTIFICATION.
EUT Report 81-E-122. 1981. ISBN 90-6144-122-6

123) Ponomarenko, M.F.
INFORMATION MEASURES AND THEIR APPLICATIONS TO IDENTIFICATION (a bibliography).
EUT Report 81-E-123. 1981. ISBN 90-6144-123-4

124) Borghi, C.A., A. Veefkind and J.M. Wetzer
EFFECT OF RADIATION AND NON-MAXWELLIAN ELECTRON DISTRIBUTION ON RELAXATION PROCESSES IN AN ATHMOSPHERIC CESIUM SEEDED ARGON PLASMA.
EUT Report 82-E-124. 1982. ISBN 90-6144-124-2

125) Saranummi, N.
DETECTION OF TRENDS IN LONG TERM RECORDINGS OF CARDIOVASCULAR SIGNALS.
EUT Report 82-E-125. 1982. ISBN 90-6144-125-0